Progress In Electromagnetics Research M, Vol. 57, 185–196, 2017

Cotton Crop Biophysical Parameter Study Using Hybrid/Compact Polarimetric RISAT-1 SAR Data

Viral A. Dave[1, *], Dipanwita Haldar[2], Rucha Dave[1], Arundhati Misra[2], and Vyas Pandey[1]

Abstract—A hybrid-polarity architecture, consisting of transmitting circular polarisation and receiving two orthogonal linear polarisation and also their relative phase, was used to calculate four Stokes parameters. Different parameters like Degree of Polarisation, Alpha angle, Entropy, Anisotropy, Radar vegetation Index and decompositions like Raney decomposition (m-δ), Freeman-2 and 3 component decompositions were derived from these hybrid data. Crop biophysical parameters viz. plant height, plant age and plant biomass of cotton crops grown under two different environments, i.e., rainfed and irrigated in Guajrat, India were studied with respect to derived polarimetric parameters. Right circular transmitted and horizontally (RH) and vertically (RV) received backscatter values show good relation with the plant height, age and biomass. RH backscatter -13 dB to -7 dB and RV backscatter from -13 to -10 dB were observed for crop biophysical parameters. Volume component of all decomposition showed strong response to the increase in height, age and biomass of the plant. Radar Vegetation index (RVI) values have also shown significant increase from 0.6 to 0.7 with increasing age of the crop. The rate of growth was slow in the initial phase, but fast post mid-July for both early and late sown cases. The polarimetric parameters were found significantly correlated to the above plant biophysical parameters.

1. INTRODUCTION

Synthetic Aperture Radar (SAR) payload operating in microwave frequency enables imaging of the surface features using active microwave remote sensing which provides cloud penetration and day-night imaging capability. SAR data are best suited for monitoring various agricultural targets as well as retrieval of its parameters due to its all-weather capability and unique sensitivity to the geometrical, structural and electrical properties of the target. This unique characteristic of C-band SAR enables applications in agriculture for rainy (*kharif*) season. The dual and quad (full) polarized data involve coherent transmission and reception of vertical or/and horizontal polarized signals (VV, VH, HV and HH) [1, 21].

Cotton is an important cash crop in India. Gujarat is the second highest cotton producing state with 36 percent of the total national production. Two different types of cotton are grown in the study area: Bacillus thuringensis (Bt) cotton grown in irrigated condition and indigenous cotton grown in rainfed condition. Dual and quad-polarized SAR data have been used for operational land cover monitoring by a number of researchers [7–9, 11–17, 22, 24, 26, 27, 29, 30]. A hybrid-polarity SAR is one in which the transmitted field is circularly polarized, and the resulting backscatter is received in two mutually coherent linear polarisations. As long as the relative phase between the received polarisations is retained, the specific choice of linear orientation does not matter. For convenience, we assume H

Received 19 December 2016, Accepted 31 May 2017, Scheduled 19 June 2017

* Corresponding author: Viral A. Dave (daveviral1@gmail.com).

[1] B.A. College of Agriculture, Anand Agricultural University, Anand, Gujarat, India. [2] Space Applications Centre, Ahmedabad, Gujarat, India.

and V polarisations. The destiny of the focused complex data is to be transformed into the four Stokes parameters, which are sufficient to capture all of the information conveyed in the backscattered EM field. This is the most that can be accomplished with any dual-polarized radar. Using these Stokes parameters, different polarimetric parameters were derived, and different decompositions were performed [2, 3, 5–7, 10, 20, 23].

This study is to establish a relation of biophysical parameter of cotton crop with polarimetric parameters derived from compact hybrid polarimetric data. Age, biomass and height were used as crop parameter, and RH and RV SLC data were used to derive polarimetric parameters like Degree of Polarisation (DoP), Radar Vegetation Index (RVI), Alpha angle, Entropy and Anisotropy along with different hybrid and model based decompositions like m-δ, Raney, Freeman 2 components, Freeman 3 components and Van Zyl decompositions. The significance of these parameters for different land covers was also established. RH and RV were used to see the backscatter response of land covers. Decompositions were used in the present study to see the different scattering mechanisms of various land covers [3, 18]. The results from a hybrid-pol data are equivalent to those from full-pol data, to the first order. Likewise, the results from a hybrid-pol will always be much better than those from single/dual pol SAR data [2].

2. HYBRID POLARIMETRIC PARAMETERS AND DECOMPOSITION

2.1. RH and RV Backscatter Response and Stokes Vector

RH and RV correspond to received electric field intensity in horizontal and vertical polarisation with the embedded cross-polar response [18]. Four Stokes parameters can be derived from RH and RV using below equation,

$$\begin{aligned} S_0 &= \langle |RH|^2 + |RV|^2 \rangle \\ S_1 &= \langle |RH|^2 - |RV|^2 \rangle \\ S_2 &= 2\mathrm{Re}\langle RH \cdot RV^* \rangle \\ S_3 &= -2\mathrm{Im}\langle RH \cdot RV^* \rangle \end{aligned}$$

* indicates the complex conjugate; $\langle \ldots \rangle$ denotes the ensemble average; Re and Im represent the real and imaginary parts of the complex field, respectively.

2.2. Degree of Polarisation-m

The ratio of the power in the polarized part of an electromagnetic wave to the total power in the electromagnetic wave is given by degree of polarisation [25].

$$m = \frac{\sqrt{S_1^2 + S_2^2 + S_3^2}}{S_0}$$
$$\delta = \tan^{-1}\left(\frac{S_3}{S_2}\right)$$

where S_0, S_1, S_2, S_3 = Stokes parameters.

This parameter is a significant distinguisher for characterizing the polarity of the backscatter. Polarity refers to the case of fully polarized, partially polarized or completely polarized cases. It ranges from 0 to 1, in which 0 indicates random or unpolarized backscatter, and 1 indicates completely polarized backscatter.

2.3. Alpha Angle (α), Entropy (H), Anisotropy (A)

The parameters alpha angle, polarimetric entropy and polarimetric anisotropy are calculated from the eigenvalues and eigenvectors of the $C2$ matrix.

$$\alpha = \frac{1}{2}\tan^{-1}\left(\frac{\sqrt{S_1^2 + S_2^2}}{-S_3}\right)$$

The alpha angle is based upon the eigenvectors and is a number indicative of the average or dominant scattering mechanism. The lower limit of 0° indicates surface scattering, and 45° indicates dipole or volume scattering, while the upper limit of 90° represents a dihedral reflector or multiple scattering.

The entropy describes polarimetric variability of the backscattering. When the target transforms the incident wave always in the same way, target entropy is the lowest; if the target changes the polarization randomly, target entropy is maximal.

Cloude and Pottier [4] proposed some parameters for interpretation of the scattering event. The first is target entropy. For a distributed target where certain scattering mechanism k_n occurs with a probability p_n, the target entropy H is defined as

$$H = -\sum_{n=1}^{3} p_n \log_3 p_n$$

Entropy (H) represents the randomness of the scattering, with $H = 0$ indicating a single scattering mechanism and $H = 1$ representing a random mixture of scattering mechanisms, i.e., a depolarizing target. Another parameter that provides useful scattering information is anisotropy, a parameter based upon the ratio of eigenvalues, which indicates multiple scatterers.

2.4. Raney (m-δ) Decomposition

Raney [20] developed this technique using basic principle as the relative phase difference between horizontally and vertically polarized backscatter signals get effect for each scattering. The total intensity is first partitioned into completely polarized and unpolarized parts using degree of polarisation. The unpolarized part is considered as volume component, and polarized part is again divided into even and odd bounce components.

$$\begin{aligned} f_{even} &= \sqrt{S_0 \cdot m \cdot \frac{1-\sin\delta}{2}} \\ f_{diffuse} &= \sqrt{S_0 \cdot (1-m)} \\ f_{odd} &= \sqrt{S_0 \cdot m \cdot \frac{1+\sin\delta}{2}} \end{aligned}$$

The components derived from this decomposition can be related to the physical processes of double-bounce, volumetric, and surface scattering ($f_{even}, f_{diffuse}, f_{odd}$), respectively. $f_{diffuse}$ is related to dominantly unpolarized backscatter which characterizes vegetation medium [2].

2.5. Freeman-2 Decomposition

The model based decomposition includes two simple scattering mechanisms, one for volume scattering, and the other is double bounce scattering. This model is a simplification of more complicated higher order scattering models [5, 18]. The Freeman-2 decomposition models the covariance matrix as two different scattering mechanisms to estimate the return power due to volume scattering and ground return.

2.6. Freeman-3 Decomposition

The observed scattering can be modeled as the linear sum of different scatterings, eg., double bounce scattering, volume scattering and surface scattering [6]. The Freeman decomposition models the covariance matrix as the contribution of three scattering mechanisms,

$$T = P_s T_{surface} + P_d T_{double} + P_v T_{volume}$$

where, P_s, P_d and P_v correspond to the power of each scattering.

$$T_{surface} = \frac{1}{1+|\beta|^2}\begin{bmatrix} 1 & \beta & 0 \\ \beta^* & |\beta|^2 & 0 \\ 0 & 0 & 0 \end{bmatrix}$$

$$T_{surface} = \frac{1}{1+|\alpha|^2}\begin{bmatrix} 1 & \alpha & 0 \\ \alpha^* & |\alpha|^2 & 0 \\ 0 & 0 & 0 \end{bmatrix}$$

$$T_{volume} = \frac{1}{4}\begin{bmatrix} 2 & 0 & 0 \\ 0 & 1 & 0 \\ 0 & 0 & 1 \end{bmatrix}$$

These are complex observables defined by Freeman and Durden for double bounce, surface scatterings and volume scattering where a canopy scatterer is modeled as a set of randomly oriented dipoles, double-bounce scattering modeled by a dihedral corner reflector, and surface or single-bounce scattering modeled by a first-order Bragg surface scatterer [6].

2.7. Radar Vegetation Index (RVI)

Radar Vegetation Index represents the vegetation on the ground and is also indicative of the vegetation vigour [13, 14]. The scaled values range from 0 to 1, where 0 represents the absence of biomass; 1 represents the high biomass; in between values vary with biomass. Urban area and waterbody have very low values for this index as the concept of biomass does not relate to these features. Although numerous experiments have been carried out to investigate the response of microwave sensors to crop growth parameters [1, 16, 28, 30], additional comprehensive studies for a variety of crops are needed to develop robust retrieval methods.

3. METHODOLOGY

3.1. Ground Data Collection

Ground truth data were collected by field survey of the study area synchronous to satellite data acquisition over the same. It includes the ground coordinates of the field with all important parameter information of crop and soil like crop type, crop age, crop vigour, crop height, leaf dimension, soil type, soil moisture, soil roughness, etc. Selection of field was based on crop type, crop area, field with more than 2 ha area preferred. In addition, ground truth also contains other land cover information like urban, water body, villages, natural vegetation and other plantations.

Crop parameters for different crops were collected viz. plant height (cm), crop biomass (gm/m^2), crop age, crop cover (%), crop vigor, etc. For hybrid cotton, plant height between 90–140 cm, biomass 900–4100 gm/m^2, age 40–110 days, crop cover 70–90% and medium to good crop vigor were observed, whereas for ingenuous cotton, plant height between 40–80 cm, biomass 300–1000 gm/m^2, age 30–70 days, crop cover 40–60% and medium to average crop vigor were observed. Area of hybrid (irrigated) cotton was more than indigenous cotton.

3.2. Hybrid SAR Data Processing and Data Analysis

Preprocessing of SAR data from RISAT is carried out using PolSARpro v5.0 and in-house developed software. The backscatter coefficients σ°_{RH} and σ°_{RV} were generated from RH & RV data, and using these backscatter coefficients, Stokes parameters were derived according to the equations described in Section 2.1. These Stokes parameters are used to derive different polarimetric parameters and decompositions.

Suitable Region of Interest (ROI) of GT points were created on different polarimetric parameters and decomposition images followed by further analysis.

4. STUDY AREA & DATA USED

4.1. Study Area

For this study, a 25 × 25 km area of Surendranagar district of Gujarat having central point at Surendranagar city with latitude 22.729103°N and longitude 71.632837°E was selected. The latitudinal extent of the area was 22.527°–22.777°N, and longitudinal extent was 71.444°–71.716°E. The study area mainly comprises agricultural land, surrounded by natural vegetation and scrub lands, one big city with a few village clusters and big water bodies (dams) with small ponds. Cotton, castor, sesame, jowar are the crops grown in *kharif* season in this area. There are two types of cotton grown viz. (i) BT cotton grown under irrigated condition (ii) Indigenous cotton grown under rainfed condition.

4.2. Data Used

RISAT-1 Hybrid (RH, RV), C-Band SAR as SLC level1 (L1) with FRS acquisition beam mode with descending right looking, 1.8 m pixel spacing with incidence angle of 32° data acquired on different dates 15th September and 11th October 2014 at different stages of crop have been used for this study. Fig. 1 shows the two date images with common area with GT route and points overlaid on it.

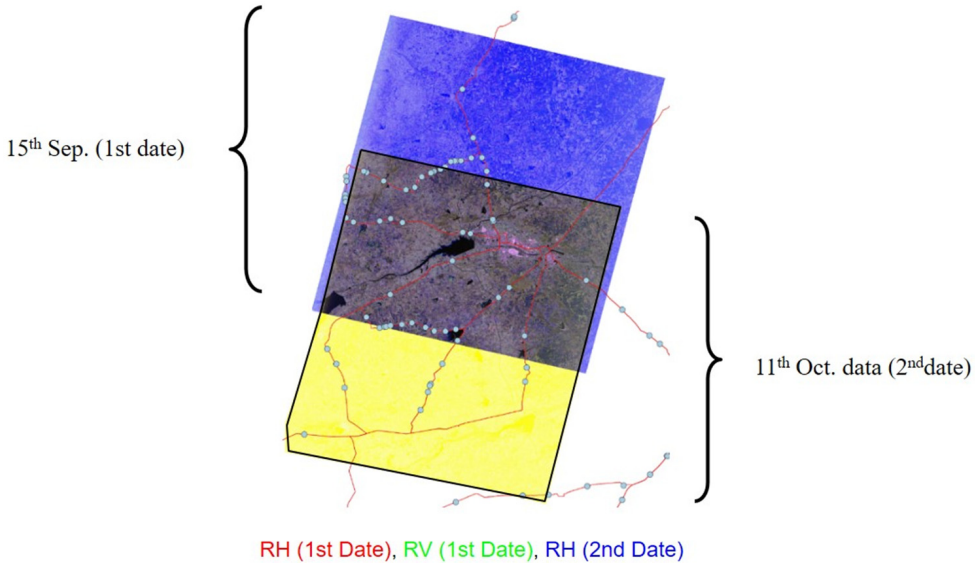

Figure 1. FCC of 2-dates stacked image with collected ground truth points and route.

5. RESULTS AND DISCUSSION

5.1. RH and RV Backscatter Response

RH backscatter values range from −16 dB to −1 dB and RV ranges from −16 dB to −6 dB as seen in Fig. 2. For various land covers, the minimum and maximum values differ according to land cover property. High intensity values more than −6 dB were observed from built-ups due to heterogeneity in those areas. Low backscatter intensity of −16 dB was identified from waterbody due to specular reflection. Indigenous cotton and castor have high backscatter values in month of October. Bt cotton shows no significant change for both dates as it was in full vegetative stage in September. Sesame and jowar also show high values and constant over time as these crops are at their maturity stage (Fig. 2(a)).

Figures 2(b)–(d) show the relation of RH and RV backscatters with different biophysical parameters of cotton crop such as biomass, age and plant height. As seen in the image, RH and RV backscatters are increased due to increasing vegetative growth of plant for all three biophysical parameters. The value for RH backscatter ranges from −13 for 40 days old crop to −7 for nearly 100

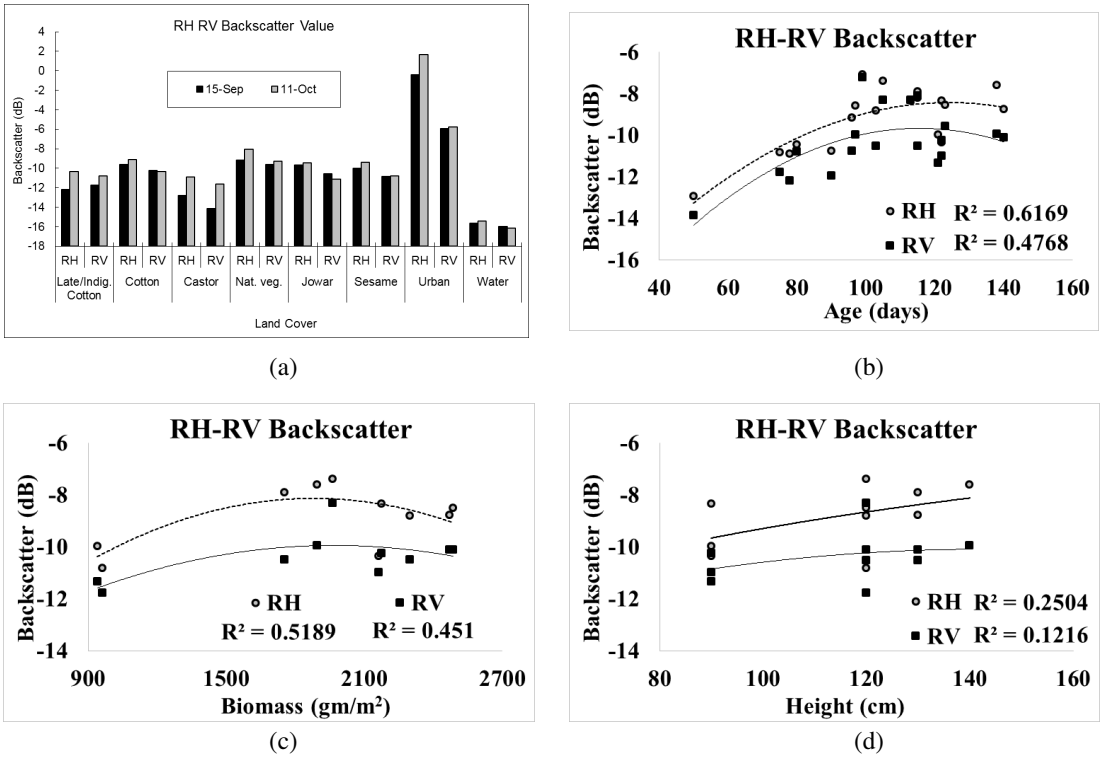

Figure 2. *RH* and *RV* backscatter response with (a) different land covers for different dates, (b) cotton crop age, (c) cotton crop biomass and (d) cotton crop height.

days old crop. Cotton plant was at its peak vegetative stage at the age of 100–120 days, and after that, boll formation and maturity stage starts. The same trend can be seen for RV backscatter. Increasing trend of backscatter for biomass and height was also observed for both *RH* and *RV* (Figs. 2(c) & (d)). Except for one or two samples, backscatter shows increasing trend with respect to height for all the samples.

5.2. Degree of Polarisation

Degree of Polarisation (DoP) was derived using in-house developed tool. As discussed earlier, in cotton crop, polarized and unpolarized return signals are random so the value of DoP is random as shown in Fig. 3. No proper relation could be established between DoP and biophysical parameters due to increased depolarisation with crop growth.

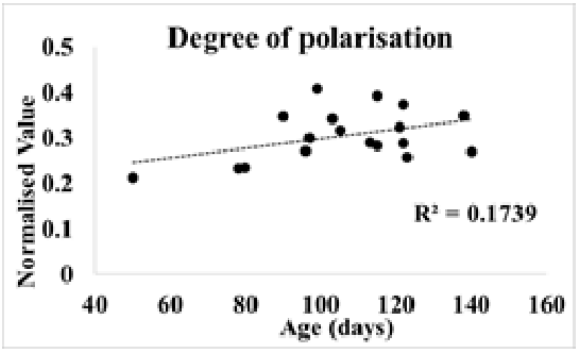

Figure 3. Age of crop with degree of polarisation.

5.3. Alpha Angle (α), Entropy (H), Anisotropy (A)

The alpha angle, entropy and anisotropy for different land covers are shown in Fig. 4. Cotton crop shows decrease in alpha angle over time as the cotton was at peak vegetative stage in September, and boll formation starts in October. In September, the castor was very small which gives low alpha angle and increases in October month as plant grows. High alpha angle is observed in the cases of jowar and sesame in the month of September and decreases in October as they are at harvesting stage. Urban area gives low values of alpha angle due to very dense area of city which acts as smooth surface, and waterbody gives higher values of angle due to undulation on surface. Natural vegetation shows high values for both dates.

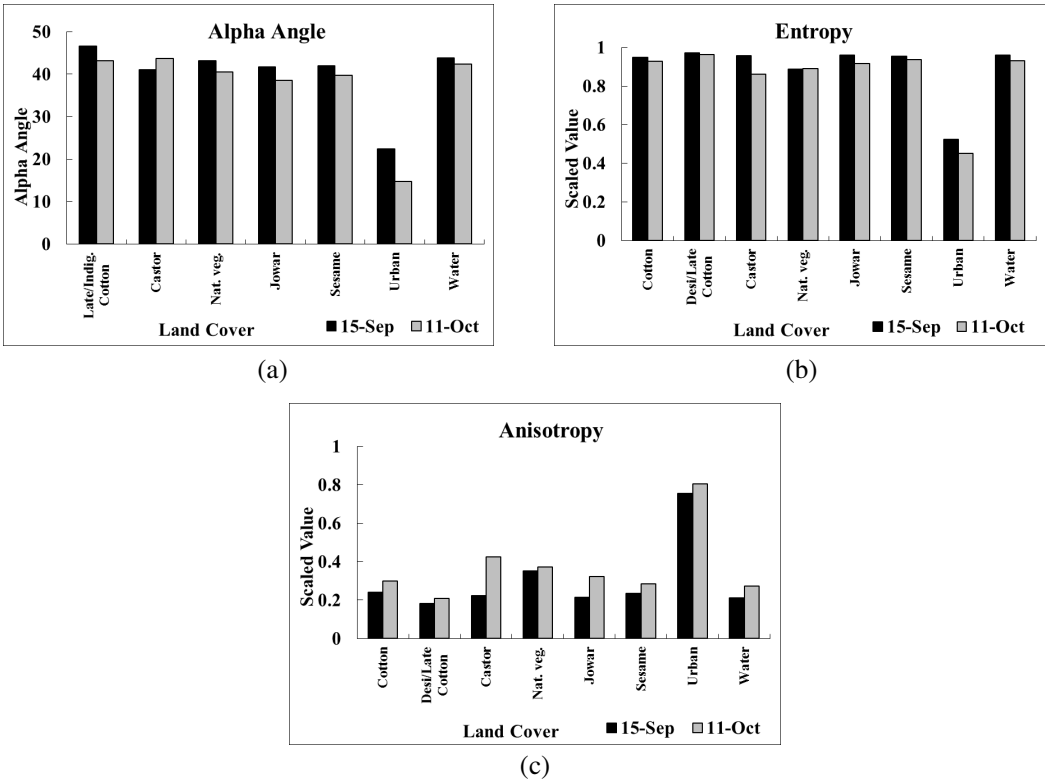

Figure 4. (a) Alpha angle (b) entropy and (c) anisotropy values for different land covers for different dates.

Waterbody such as river and sea has single scattering mechanism which gives low entropy value. Turbulence in water surface due to rain gives high entropy in this case. Urban areas have mixing scattering mechanism which gives low values of entropy of 0.4. Entropy for all the crops is very high with values more than 0.85. Urban area has high value of anisotropy. Other land cover gives lower value of anisotropy of 0.2–0.4.

5.4. 5.4 m-δ and Raney Decomposition

Crops and natural vegetation have high volume which results in to higher value of diffuse component for both m-δ and Raney decompositions. As the crop grows, the volume of crop increases, so as diffuse component for cotton, castor, jowar, sesame and natural vegetation. For urban area, even component gives higher value which represents high double bounce scattering. For water, diffuse component is observed to be higher than others due to undulated surface during rainy season (Fig. 5).

Figure 6 shows the relation of crop biophysical parameters of cotton crop with volume component of m-δ and Raney decompositions. The highest value of volume component is achieved at the age of nearly

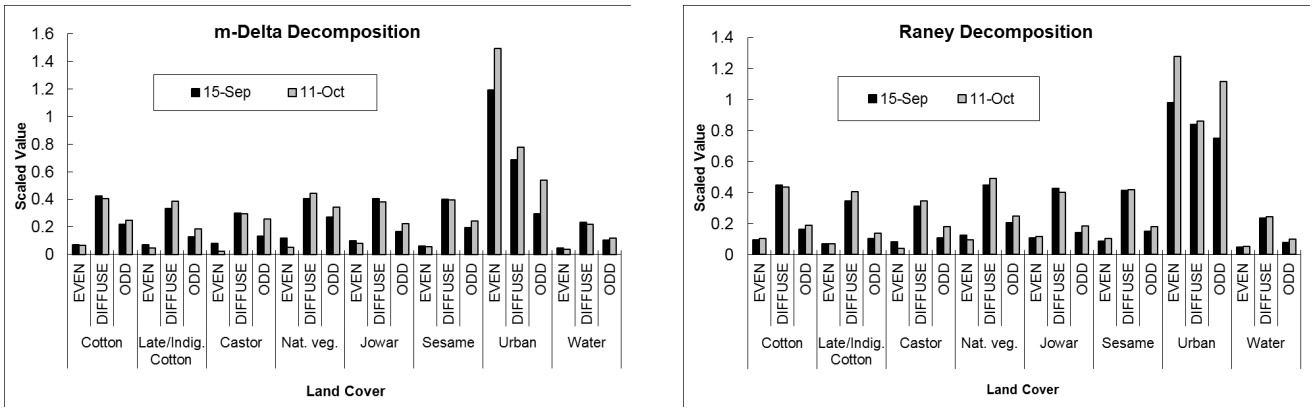

(a) (b)

Figure 5. (a) m-δ and (b) Raney decomposition value for different land cover.

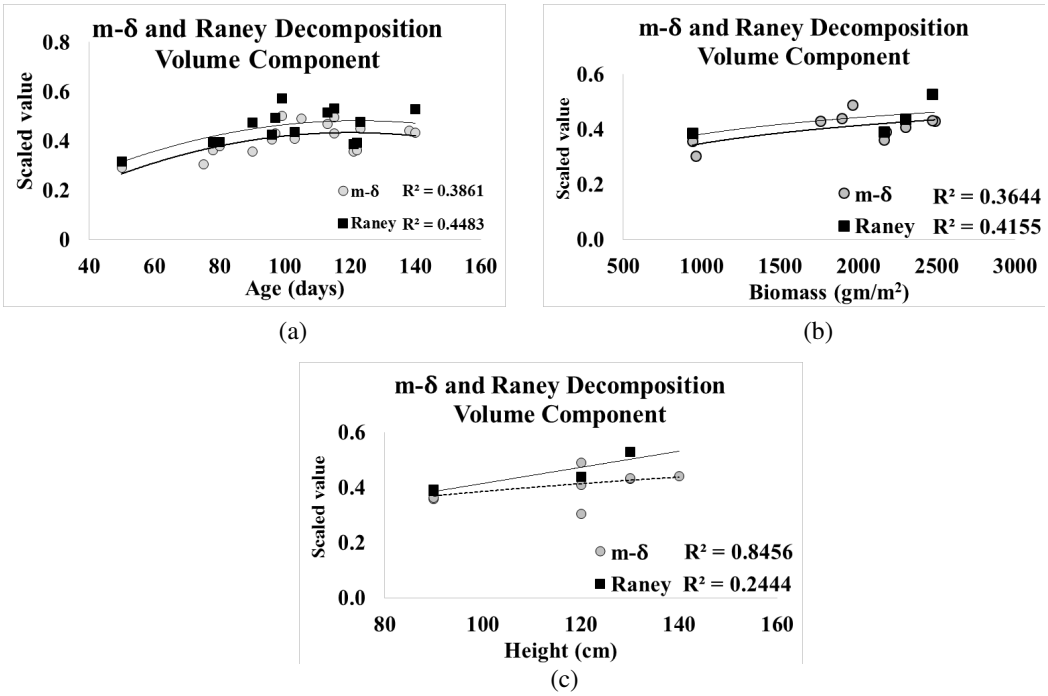

Figure 6. m-Delta and Raney decomposition volume component relation with cotton crop. (a) Age, (b) biomass and (c) height.

100–120 days when crop is at its peak vegetative stage for both the decompositions (Fig. 6(a)). Raney decomposition shows significant response of volume component with biomass and height compared to m-Delta decomposition (Figs. 6(b), (c)). In Fig. 7, m-δ decomposition image shows different crop dominating areas and changes over time. Color of images turning from green to blue shows dominating scattering component as in the first image volume component is high, and in second date image surface component is increasing as crop reaches its maturity stage exposing surface.

5.5. Freeman-2, Freeman-3 and Van-Zyl Decomposition

These three model based decompositions are derived from C3 (pseudo) matrix. Freeman-2 and Freeman-3 decomposition values are mostly similar for all the land covers. Value of volume component increases

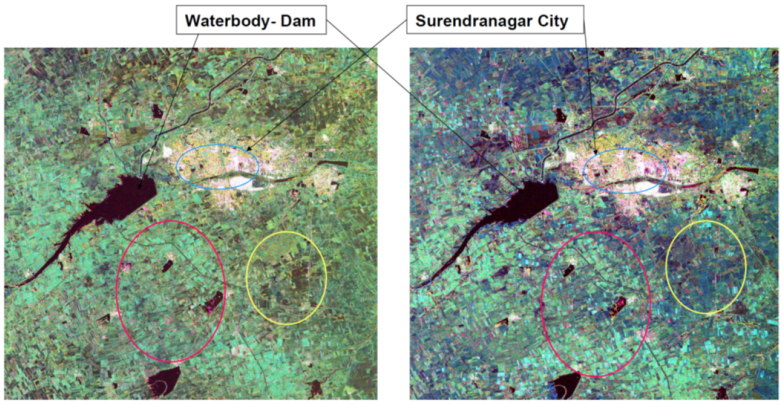

Figure 7. m-δ decomposition image (Even Component), (Diffuse Component), (Odd Component) for two date (15th Sep. 2015 and 11th Oct. 2015) showing cotton area (red circle) and sesame and jowar area (yellow circle).

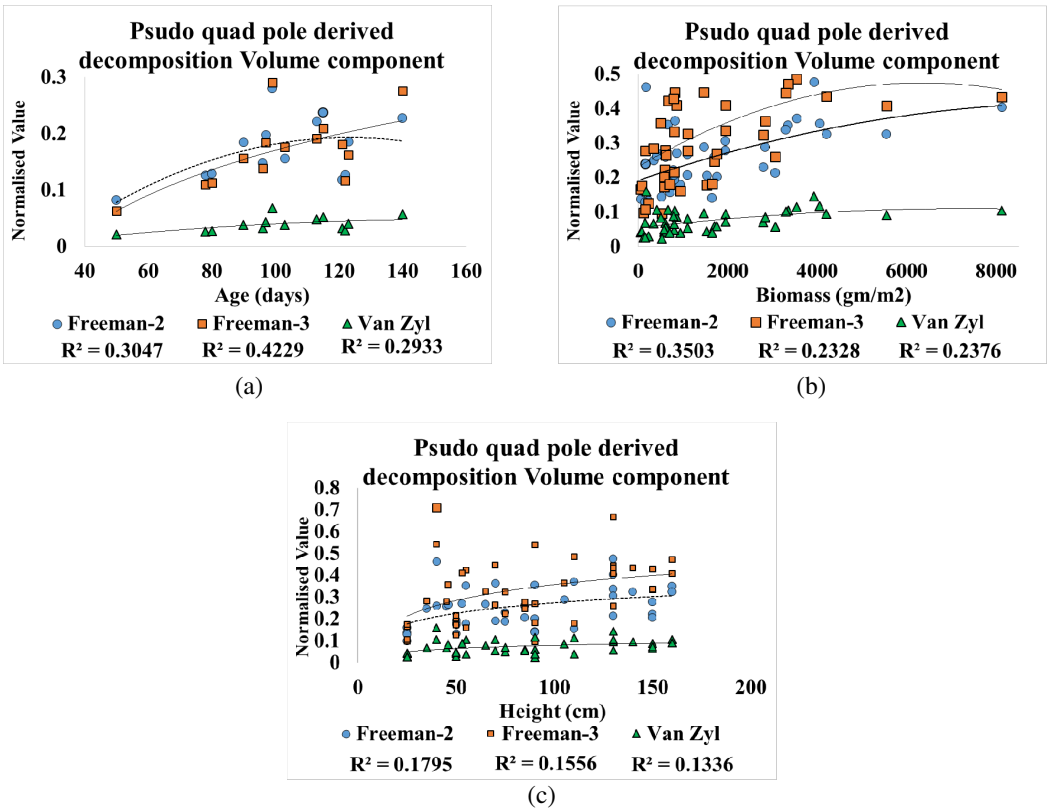

Figure 8. (a) Age, (b) biomass and (c) height of crop relation with Freeman-2, Freeman-3 and Van Zyl decomposition Volume component.

for cotton, castor, indigenous cotton and natural vegetation because of the growth of vegetation with respect to age. For built-up areas in urban, the double bounce scattering was high due to vertical structures of the buildings [4–6].

The relation of volume component of three different decompositions Freeman-2, Freeman-3 and Van Zyl with age, biomass and height of cotton crop is shown in Fig. 8. Taking the same signature points for all the three decompositions, it is observed that Freeman-3 gives better result than other two decomposition models for cotton crop.

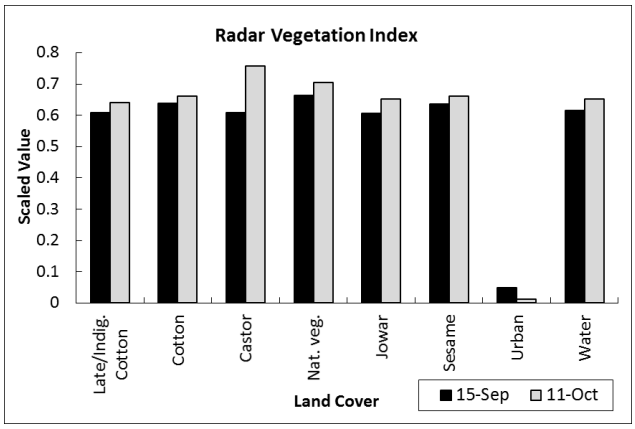

Figure 9. Radar vegetation index value for different land cover.

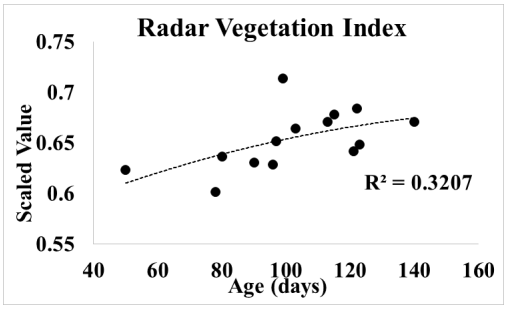

Figure 10. Age of crop relation with RVI.

5.6. Radar Vegetation Index (RVI)

There is minor increase in RVI values observed as the crop was at its high vegetative and boll formation stage in September and October, respectively. In the case of indigenous (*desi*) cotton which is late sown, significant increases in the RVI values were observed. Castor sown in late July or early August gives increase in RVI value from 0.6 to 0.75. Jowar, sesame and natural vegetation show constant values of RVI over time as in September they reached their maturity phase, so there was no significant vegetation increase in these crops so as in RVI. Very low RVI ranging from 0.01 to 0.25 with mean of 0.05 in September and 0 to 0.1 with mean of 0.013 in October is for urban area. In general, all vegetative land covers signify high RVI values as seen in Fig. 9. Fig. 10 shows the relation between Radar Vegetation Index with the age of cotton crop. RVI value of 0.6 to 0.7 is attained at the age of 100–120 days when crop is at its highest vegetative stage.

6. CONCLUSION

Hybrid polarity backscatters RH and RV show high correlation with crop parameters, especially in RH domain, and the values were significant in relation with crop biophysical parameters. Cotton crop polarized and unpolarized return signals are random, so the value of DoP was random, and no proper relation can be found between DoP and the age of crop. Raney based m-delta decomposition yielded promising results in terms of plant biophysical parameters such as biomass, age plant and height. The rate of growth was slow in the initial phase but observed fast post mid-July for both early and late sown cases which were reflected in terms of polarimetric parameters for the above plant biophysical parameters. C2 based parameters yielded sensible results but converting C2 to C3 for getting full-pol decomposition did not yield expected results [19]. The Freeman 2 and Van Zyl decomposition did not add any significant result to the Raney decomposition, but Freeman 3 component decomposition shows better results than the other two. Radar vegetation index also shows promising response as the age of crop is increased. Multidate data have been used for understanding temporal behavior of cotton crop biophysical parameters with respect to polarimetric parameters. Radar based vegetation indices (RVI) are explored to establish correlation with biophysical parameters.

ACKNOWLEDGMENT

The authors are grateful to Dr. N. C. Patel, Vice Chancellor, Anand Agricultural University and Dr. K. B. Kathiria, Director of Research, Anand Agricultural University for his support and encouragement during the period of investigation. The authors are also thankful to Shri Tapan Misra, Director, Space Applications Centre, ISRO for providing opportunity to carry out this work and guidance during the study.

REFERENCES

1. Bouvet, A., T. L. Toan, and N. Lam-Dao, "Monitoring of the rice cropping system in the Mekong Delta using ENVISAT/ASAR dual polarisation data," *IEEE Trans. Geosci. Remote Sens.*, Vol. 47, No. 2, 517–526, Feb. 2009.
2. Charbonneau, F. J., B. Brisco, R. K. Raney, H. McNairn, C. Liu, P. Vachon, J. Shang, R. DeAbreu, C. Champagne, A. Merzouki, and T. Geldsetzer, "Compact polarimetry overview and applications assessment," *Can. J. Remote Sens.*, Vol. 36, Suppl. 2, S298–S315, 2010.
3. Cloude, S. R., D. G. Goodenough, and H. Chen, "Compact decomposition theory," *IEEE Geoscience and Remote Sensing Letters*, Vol. 9, No. 1, Jan. 2012.
4. Cloude, S. R. and E. Pottier, "A review of target decomposition theorems in radar polarimetry," *IEEE Geoscience and Remote Sensing Letters*, Vol. 34, No. 2, Mar. 1996.
5. Freeman, A., "Fitting a two component scattering model to polarimetric SAR data from forests," *IEEE Trans. Geosci. Remote Sens.*, Vol. 45, No. 8, 2583–2592, 2007.
6. Freeman, A. and S. L. Durden, "A three-component scattering model for polarimetric SAR data," *IEEE Trans. Geosci. Remote Sens.*, Vol. 36, No. 3, 963–973, 1998.
7. Freeman, J., J. D. Villasenor, H. P. Klein, and J. Groot, "On the use of multi-frequency and polarimetric radar backscatter features for classification of agricultural crops," *Int. J. Remote Sensing*, Vol. 15, No. 9, 1799–1812, 1994.
8. Haldar, D., A. Das, S. Mohan, O. Pal, R. S. Hooda, and M. Chakraborty, "Assessment of L band SAR data at different polarisation combinations for crop and other landuse classification," *Progress In Electromagnetics Research B*, Vol. 36, 303–321, 2012.
9. Haldar, D., P. Rana, M. Yadav, R. S. Hooda, and M. Chakraborty, "Time series analysis of co-polarisation phase difference (PPD) for winter field crops using polarimetric C-band SAR data," *International Journal of Remote Sensing*, Vol. 37, No. 16, 3753–3770, DOI: 10.1080/01431161.2016.1204024.
10. Jaan, P., E. C. Koeniguer, and M. T. Hallikainen, "Alternatives to target entropy and alpha angle in SAR polarimetry," *IEEE Trans. Geosci. Remote Sens.*, Vol. 47, No. 7, Jul. 2009.
11. Jackson, T. J. and T. J. Schmugge, "Vegetation effects on the microwave emission of soils," *Remote Sens. Environ.*, Vol. 36, No. 3, 203–212, Jun. 1991.
12. Jin, Y. Q. and C. Liu, "Biomass retrieval from high-dimensional active/passive remote sensing data by using artificial neural networks," *Int. J. Remote Sens.*, Vol. 18, No. 4, 971–979, 1997.
13. Kim, Y. J. and J. Van Zyl, "A time-series approach to estimate soil moisture using polarimetric radar data," *IEEE Trans. Geosci. Remote Sens.*, Vol. 47, No. 8, 2519–2527, Aug. 2009.
14. Kim, Y., T. Jackson, and R. Bindlish, "Radar vegetation index for estimating the vegetation water content of rice and soybean," *IEEE Geoscience and Remote Sensing Letters*, Vol. 9, No. 4, Jul. 2012.
15. Lee, J. S., M. R. Grunes, and E. Pottier, "Quantitative comparison of classification capability: Fully polarimetric versus dual-and single-polarisation SAR," *IEEE Trans. Geosci. Remote Sens.*, Vol. 39, No. 11, 2343–2351, 2001.
16. Maity, S., C. Patnaik, and S. Panigrahy, "Analysis of temporal backscattering of cotton crops using a semi-empirical model," *IEEE Trans. Geosci. Remote Sens.*, Vol. 42, No. 3, 577–587, Mar. 2004.
17. Panigrahi, R. K. and A. K. Mishra, "An unsupervised classification of scattering behaviour using hybrid polarimetry," *IET Radar, Sonar & Navigation*, 270–276, Vol. 7, No. 3, Mar. 2013.
18. Pottier, E., J. S. Lee, and F. F. Laurent, "Advanced concepts," PolSARpro v3.0 – Lecture Notes.
19. Raney, R. K., "Comparing compact and quadrature polarimetric SAR performance," *IEEE Geoscience and Remote Sensing Letters*, Vol. 13, No. 6, June 2016.
20. Raney, R. K., "Decomposition of hybrid-polarity SAR data," *IEEE Trans. Geosci. Remote Sens.*, Vol. 45, No. 11, November 2007.
21. Raney, R. K., "Hybrid-polarity SAR architecture," *IEEE Trans. Geosci. Remote Sens.*, Vol. 45, No. 11, Nov. 2007.

22. Schotten, C. G. J., W. W. L. Van Rooy, and L. L. F. Janssen, "Assessment of the capabilities of multi-temporal ERS-1 SAR data to discriminate between agricultural crops," *Int. J. Remote Sensing*, Vol. 16, No. 14, 2619–2637, 1995.
23. Shivany, R., M. Chabert, and J. Y. Tourneret, "Estimation of the degree of polarization for hybrid/compact and linear dual-pol SAR intensity images: Principles and applications," *IEEE Geoscience and Remote Sensing Letters*, Vol. 51, No. 1, Jan. 2013.
24. Skriver, H., T. S. Morten, and A. G. Thomsen, "Multitemporal C- and L-band polarimetric signatures of crops," *IEEE Trans. Geosci. Remote Sens.*, Vol. 37, No. 5, 2413–2429, 1999.
25. Thota, S., H. S. Srivastava, P. K. Sharma, K. Dhiraj, and P. Patel, "Study of hybrid polarimetric parameters generated from Risat-1 SAR data for various land cover targets," *International Journal of Advancement in Remote Sensing, GIS and Geography (IJARSGG)*, Vol. 3, No. 1, 32–42, 2015.
26. Toan, L. T., H. Laur, E. Mougin, and A. Lopes, "Multitemporal and dual-polarisation observations of agricultural vegetation covers by X-band SAR images," *IEEE Trans. Geosci. Remote Sens.*, Vol. 27, 709–717, Nov. 1989.
27. Toan, L. T., F. Ribbes, L. F. Wang, N. Floury, K. H. Ding, J. A. Kong, M. Fujita, and T. Kurosu, "Rice crop mapping and monitoring using ERS-1 data based on experiment and modeling results," *IEEE Trans. Geosci. Remote Sens.*, Vol. 35, 41–56, Jan. 1997.
28. Tucker, C. J., "Red and photographic infrared linear combinations for monitoring vegetation," *Remote Sens. Environ.*, Vol. 8, No. 2, 127–150, May 1979.
29. Turkar, V., R. Deo, Y. S. Rao, S. Mohan, and A. Das, "Classification accuracy of multi-frequency and multi-polarisation SAR images for various land covers," *IEEE Journal of Selected Topics in Applied Earth Observations and Remote Sensing*, Vol. 5, No. 3, 936–941, Jun. 2012.
30. Wigneron, J. P., P. Ferrazzoli, A. Olioso, P. Bertuzzi, and A. Chanzy, "A simple approach to monitor crop biomass from C-band radar data," *Remote Sens. Environ.*, Vol. 69, No. 2, 179–188, Aug. 1999.